Available online at www.sciencedirect.com
SCIENCE DIRECT®
Bioelectrochemistry 61 (2003) 1–8
Bioelectrochemistry
www.elsevier.com/locate/bioelechem

Electrochemistry of nano-scale bacterial surface protein layers on gold

Marlene Handrea[a], Mario Sahre[a], Angela Neubauer[b], Uwe B. Sleytr[b], Wolfgang Kautek[a,*]

[a] *Laboratory for Thin Film Technology, Federal Institute for Materials Research and Testing, Unter den Eichen 87, Berlin D-12205, Germany*
[b] *Centre for Ultrastructure Research, Ludwig Boltzmann Institute for Molecular Nanotechnology, Universität für Bodenkultur Wien Gregor Mendel-Strasse 33, Wien A-1180, Austria*

Received 19 September 2002; received in revised form 5 March 2003; accepted 18 March 2003

Abstract

The mechanism of the recrystallization of nano-scale bacterial surface protein layers (S-layers) on solid substrates is of fundamental interest in the understanding and engineering of biomembranes and e.g. biosensors. In this context, the influence of the charging state of the substrate had to be clarified. Therefore, the electrochemical behaviour of the S-layers on gold electrodes has been investigated by in-situ electrochemical quartz microbalance (EQMB) measurements, scanning force microscopy (SFM) and small-spot X-ray photoelectron spectroscopy (SS-XPS) of potentiostatically emersed substrates. It was shown that the negatively charged bonding sites of the S-layer units (e.g. carboxylates) can bond with positively charged Au surface atoms in the positively charged electrochemical double layer region positive of the point of zero charge (~ -0.8 V vs. saturated mercury-mercurous sulphate electrode). Surface conditions in other potential regions decelerated the recrystallization and fixation of S-layers. Time-resolved in-situ and ex-situ measurements demonstrated that two-dimensional S-layer crystal formation on gold electrodes can occur within few minutes in contrast to hours common in self-assembled monolayer (SAM) generation. These results proved that the recrystallization and fixation of 2D-crystalline S-layers on an electronic conductor can be influenced and controlled by direct electrochemical manipulation.

Keywords: S-layers crystallization; Gold; Electrochemical quartz microbalance; Scanning force microscopy; XPS

1. Introduction

Two-dimensional crystalline bacterial cell surface layers (S-layers) on solid substrates are of fundamental and technological interest in biotechnology [1], biomineralization [2], biosensorics [3,4], and bottom-up nanostructuring technologies [5,6].

The controlled immobilisation of such molecules on surfaces is an essential requirement in supramolecular engineering and macromolecular nanotechnology. The self-assembly method has been recognized as one of the most attractive approaches to creating well-defined functional molecular layers on solid surfaces. Thus, this intrinsic property of the S-layer to form monolayers at solid surfaces at the air/water interface is the key feature for functionalising surfaces [4,7]. When aiming to create biofunctional structures on a solid support, biomolecules need to be kept in their native state so that they can continue to function. Also important is the specificity of the interaction between macromolecules and the functionalised surface. According to this principle, the macromolecules may be bound to an S-layer in dense crystalline packing. Specific binding of biomolecules on S-layer lattices may be induced by different non-covalent as well as covalent forces [7].

It is important to note that the inner and outer surfaces of the S-layer lattices are highly anisotropic structures. In general, the inner surface is less hydrophobic than the outer one and reveals a net negative surface charge (excess of carboxylic acid groups) in comparison to the outer surface that exhibits a charge-neutral characteristics (equimolar amount of carboxylic acid and amino groups) [4,7]. In most S-layer lattices, the constituent subunits interact with each other and with the supporting cell envelope layer by a combination of non-covalent forces including hydrogen or ionic bonds, and hydrophobic or electrostatic interactions. The orientation of the protein arrays recrystallized at interfaces is determined by the anisotropy of the physico-chemical surface properties of S-layer lattices [7]. Electron microscopical examinations revealed that recrys-

* Corresponding author. Tel.: +49-30-8104-1822; fax: +49-30-8104-1827.
E-mail address: wolfgang.kautek@bam.de (W. Kautek).

1567-5394/$ - see front matter © 2003 Elsevier B.V. All rights reserved.
doi:10.1016/S1567-5394(03)00047-1

tallized S-layers were oriented with their charge-neutral, more hydrophobic outer face towards hydrophobic solid surfaces, such as gold.

The hydrophilicity or the hydrophobicity characteristics of the gold surfaces are also important and can affect the protein recrystallization process. In general, highly hydrophobic surfaces are better suited for the formation of large-scale closed S-protein monolayers than less hydrophobic or hydrophilic supports [8]. An exception is the *Bacillus sphaericus* CCM 2177 used in the present study, which can form large monocrystalline domains on hydrophilic surfaces [9]. The pure gold can attain both a hydrophilic and hydrophobic surface depending on the potential [10].

The mechanism of the recrystallization of nano-scale bacterial surface protein layers (S-layers) on solid substrates is of fundamental interest in the understanding and engineering of biomembranes and e.g. biosensors. Therefore, the influence of the charging state of the substrate had to be clarified. In this study, SFM in a fluid cell and small-spot-X ray photoelectron spectroscopy (SS-XPS) were employed to investigate the recrystallization and fixation of the S-layer proteins on the gold in an ex-situ mode. More importantly, the possibilities of electrochemical manipulation of the metal surface was investigated in order to generate and control direct bond formation between protein molecules, their crystal phase, and the surface metal atoms. The electrochemistry of these processes was investigated in-situ by an electrochemical quartz crystal microbalance (EQMB) with the capability to measure mass changes in the nanogram order at the electrode surface/electrolyte interfaces.

2. Experimental

A computerized electrochemical quartz microbalance system (CHI 440) was used for recording the frequency change during in-situ S-layer recrystallization processes. The EQMB electrodes with a fundamental resonant frequency of 8 MHz and 13.7 mm diameter were of the AT-cut type, with optically polished surfaces coated on both sides with 200 nm thick gold layer, 5 mm diameter, over a thin chromium adhesion mediator film. Since the EQMB operated in time-resolved mode, the frequency difference of the working crystal and the reference crystal was measured. The EQMB experiment relies on the calculation of mass change (Δm) at the quartz crystal vs. frequency change (Δf).

$$\frac{\Delta m}{\Delta f} = -\frac{A\sqrt{\rho_Q \mu_Q}}{2f_0} \quad (1)$$

where A is the piezoelectrically active area, μ_Q is the shear modulus of quartz, ρ_Q is the quartz density and f_0 is the resonant frequency. The density of the crystal was 2.648 g cm^{-3} and the shear modulus 2.947×10^{11} g cm^{-1} s^{-2}. $\Delta m/\Delta f$ for the 8 MHz crystal was 1.34 ng/Hz with an active area of 0.20 cm^2.

The EQMB cell consisted of three round Teflon pieces. The top component was the cell top to hold the reference and counter electrodes. The centrepiece was the cell compartment for the electrolyte. The bottom served for mounting. The total height was 37 mm with a diameter of 35 mm. A gold wire served as counter electrode and a saturated mercury-mercurous sulphate electrode (MSE) as reference electrode (+0.66 V vs. normal hydrogen electrode). All electrode potentials are reported vs. the MSE. The stability of the EQMB in air and water was checked before each measurement. The frequency shift at 22 °C during 400 s was less than 1 Hz in both conditions.

EQMB measurement only yield integral mass values and cannot give any data about morphological changes and the homogeneity of deposits. This deficiency was amended by the combination of the preparation of electrodes in a standard potentiostatic three-electrode cell under potential-controlled emersion and ex-situ investigation by a scanning force microscope in contact mode in a standard fluid cell. This procedure yields data which are representative for the electrochemically controlled interface when care is taken that the electrochemical double layer is not discharged during the emersion procedure under potentiostatic control [11,12].

The electrolytes were prepared with double-distilled water and analytical grade reagents. All experiments were performed at room temperature (22 °C). The electrodes were rinsed with ethanol and water, and finally dried in a stream of nitrogen gas. After that, electrochemical cleaning was performed in the electrolyte borate buffer (100 mM $NaClO_4$, 1 mM H_3BO_3, adjusted to pH 9 with NaOH) used for the further S-layer crystallization. The repeated cycling in the borate buffer was done in the potential range from −1.4 to 0.4 V at a scan rate of 50 mV s^{-1} in order to obtain a clean and reproducible gold surface. A dosimeter (Metrohm 655) was used to inject the protein and the $Ca(ClO_4)_2$ solutions into the EQMB cell at a constant flow rate.

The S-layers are mostly composed of a single protein or glycoprotein species. Typically, S-layer proteins possess a high content of acidic and hydrophobic amino acids. The S-layer protein units (from *B. sphaericus* CCM 2177) with the molar mass of 132000 g mol^{-1} (Table 1) and square lattice symmetry was prepared by extracting from bacterial cell

Table 1
S-layer properties (*B. Sphaericus* CCM 2177)

Lattice type	Square
Base vectors of the unit cell	$a = b = 13.1 \pm 0.4$ nm
Molar mass of subunits	132,000 g mol^{-1}
Number of subunits per unit cell	4
Binding sites	~ 1.6/nm^2 (−COOH)
Area per unit cell	$A = 172$ nm^2
Pore diameter	4–5 nm
Surface coating	510 ng/cm^2

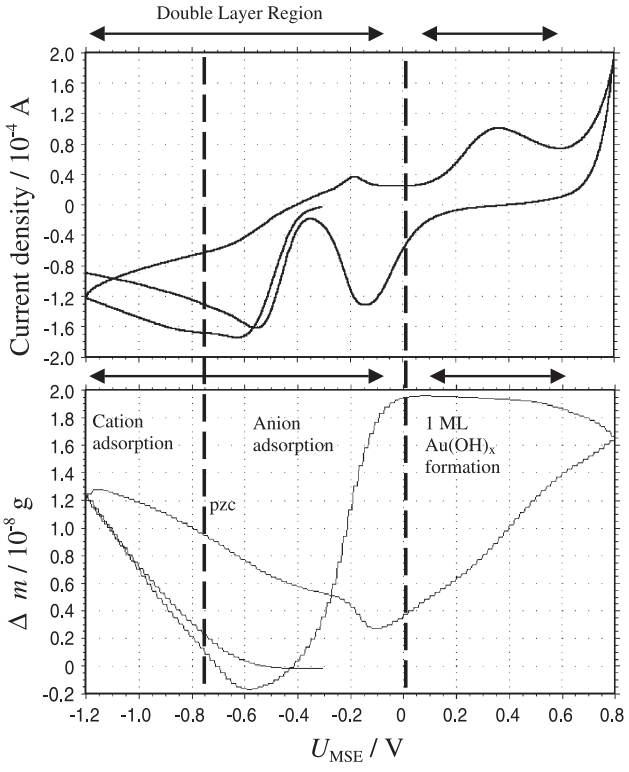

Fig. 1. Cyclic voltammogram and in-situ EQMB measurement on a Au electrode (Au on quartz crystal) in crystallization buffer for SbpA (borate buffer with 10 mM $Ca(ClO_4)_2$, pH 9). Δm: mass change derived from EQMB frequency change.

using guanidine hydrochloride (GHCl) 5 M. The GHCl extract (the isolated S-layer subunits) was dialysed against water (MilliQ). Dialysis was stopped after 2 h and with regard to the volume used, a small amount of GHCl of about 0.2–0.5 mM GHCl remained in the dialysed protein solution. It was stored under refrigeration.

The recrystallisation of the S-layer protein on the gold substrate was carried out at room temperature in the borate buffer. Solutions of $Ca(ClO_4)_2$ and S-layer units were injected independently form each other to yield concentrations of 10 and 0.001 mM, respectively.

Scanning force microscopy (SFM) in contact mode with loading forces in the range of 0.1–0.2 nN in a fluid cell is the only tool that allows the imaging of the S-layer protein monolayers on solid supports at molecular resolution [13]. A SFM (Nanoscope III Multi-Mode, Digital Instruments) equipped with a liquid cell and a 120 μm scanner and oxide-sharpened silicon nitride tips (Nanoprobes, Digital Instruments) with a nominal spring constant of 0.06 N/m were used for SFM investigations. Imaging was carried out in contact mode under liquid (100 mM NaCl). The applied force was maintained at <1 nN and the scan rate typically 5.1 Hz at a scan size of 1×1 μm. Particular care was taken to avoid dewetting of the samples when mounting them into the fluid cell.

Small-spot XPS (SSXPS) measurements (Surface Science Lab S-Probe) were performed with a monochromated Al–K_α (1486.6 eV) X-ray radiation. The emitted photoelectrons were detected using a hemispherical analyser at a pass energy of 50 eV for the C1s, O1s, N1s high-resolution XPS peaks at a take-off angle of 35°. The energy resolution at 50 eV was 0.88 V, and was estimated from the full width at half maximum (FWHM) of the XPS $Ag3d_{5/2}$ of a pure Ag target. The analysed area was 0.2 mm^2. The measured peaks were deconvoluted assuming Gaussian profiles.

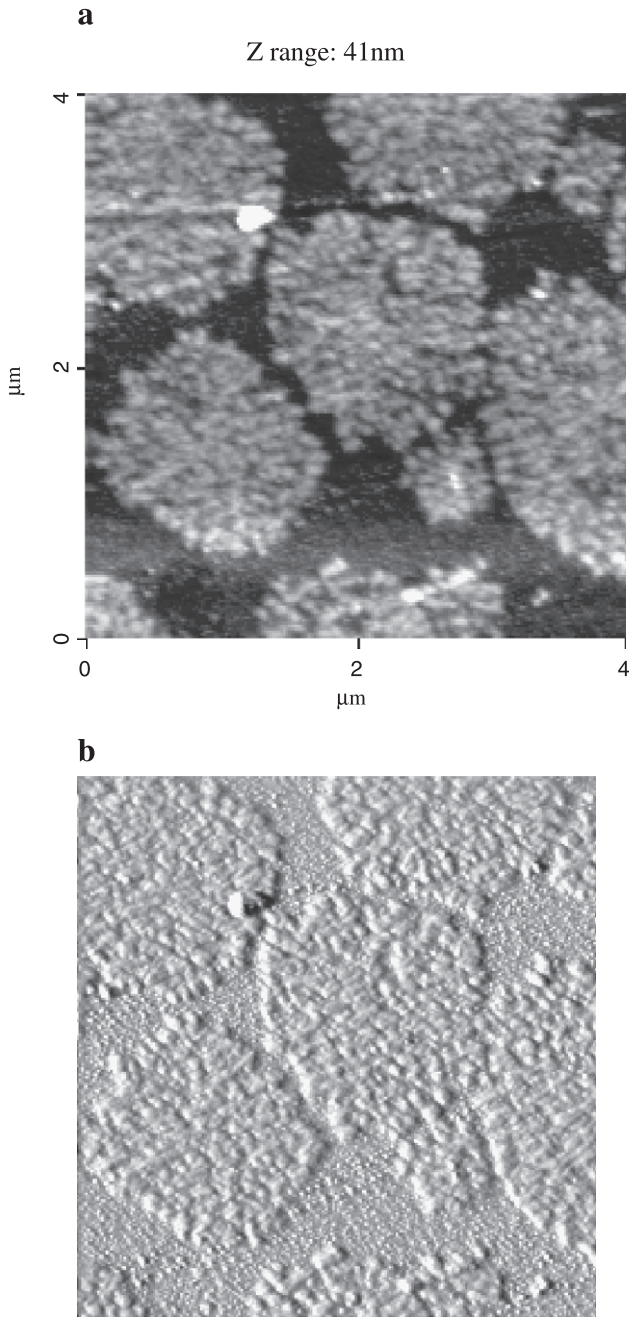

Fig. 2. SFM images of gold electrodes (Au on quartz crystal) after S-layer recrystallization processing at -1.2 V (vs. MSE). (a) SFM height signal, (b) SFM sensor signal.

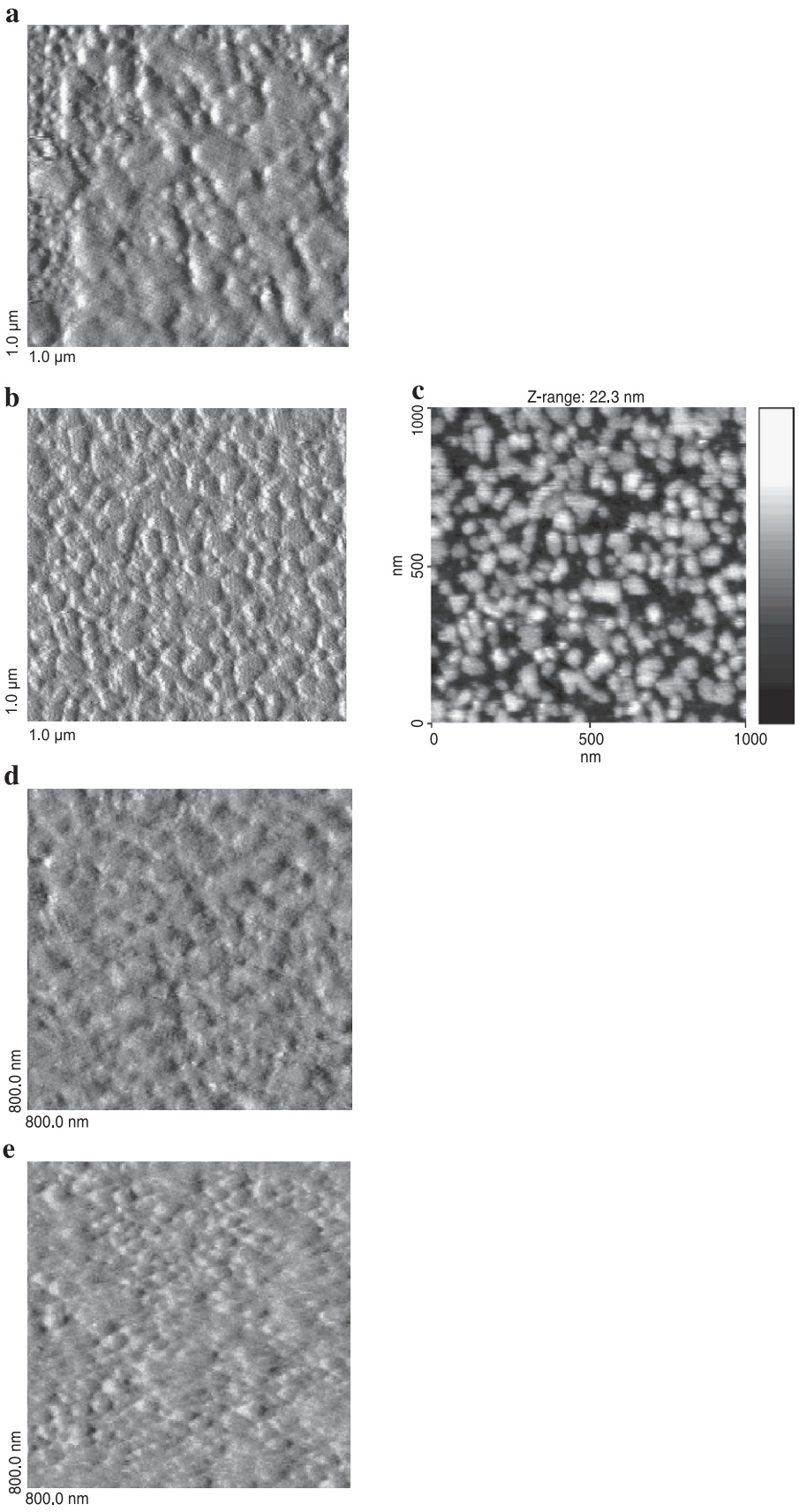

Fig. 3. SFM images (sensor signals) of gold electrodes (Au on quartz crystal) after S-layer recrystallisation processing at: (a) − 1.2 V, (b) − 0.8 V, (c) − 0.8 V (SFM height signal; average height from histogramme 4.6 nm), (d) − 0.2 V; (e) + 0.4 V (vs. MSE).

3. Results and discussion

The formation of a protein monolayer on gold is strongly dependent on several factors as cleanliness and structure of gold prior to modification, the nature of the buffer used for the S-layer recrystallization, the concentration, the temperature, the pH value, etc. Buffer components may interfere with the fixation reactions of S-layer units on a metal. Therefore, the borate buffer electrolyte with the $Ca(ClO_4)_2$ linking additive used for the recrystallization of the S-layer units of *B. sphaericus* CCM 2177 (SbpA) was investigated in a EQMB. Current–potential (I–U) and mass change–potential curves (Δm–U) were simultaneously recorded (Fig. 1). The double layer (*dl*) region was in the potential range from ca. −1.2 to 0 V, with the point of zero charge (*pzc*) at c. −0.8 V. The respective excess charges in form of ionic adsorption is indicated in Fig. 1. An anodic potential scan from −1.2 to −0.1 V shows that the double layer becomes lighter, i.e. that the solvated cations such as $Ca^{2+}(H_2O)_x$ and $Na^{+}(H_2O)_x$ in the negative double layer are heavier than the borate, perchlorate and hydroxide anions in the positively charged double layer. A complication in the interpretation may be the fact that negative currents at $U < -0.3$ V indicate the concurrent reduction of oxygen traces. The formation of a $Au(OH)_x$ monolayer in the region >0 V causes a mass increase, which is further continued into the Au/OH place exchange region [10] ($U > +0.6$ V). The cathodic excursion from the $Au(OH)_x$ monolayer region causes mass reduction by the hydroxide/oxide removal indicated by the negative current peak.

Based on the EQMB study (Fig. 1) four characteristic potentials were selected for further morphological and time-resolved investigations: −1.2 V, in the negatively charged *dl*-region with the cation excess and parallel oxygen reduction, −0.8 V, near the *pzc* with parallel oxygen reduction, −0.2 V, in the positively charged *dl*-region with the anion excess, and +0.4 V, in the monolayer oxide region, respectively.

In the negatively charged *dl*-region with the cation excess and parallel oxygen reduction at −1.2 V, S-layers do not form homogeneous monolayer crystals (Figs. 2 and 3a). Isolated fractal clusters of about 2000 nm diameter arranged around few sites. The thickness of these is of the order of 10–18 nm (Fig. 2a). That means that multilayers are formed. The surface only allowed the survival of very few protein crystal nuclei, which could grow laterally. The bonding situation of the S-layer units and/or clusters to the cation-covered negatively charged Au surface is disadvantageous. One can assume that those bonding sites (e.g. $-COO^{-}$) on the proteins that interact with the Ca^{2+} ions are already saturated before the adsorption step. The *B. sphaericus* CCM 2177 type under study actually exhibits an anisotropy in respect to an excess of carboxylate groups in lateral direction vs. the top and bottom side of the units. The protein amino groups ($-NH_2$), on the other hand, are neutral at pH 9 and should not undergo major ionic and covalent bonding to Au. Other phenomena, however, appear to be more dominant in respect to the poor bonding condition. One is the net charge transfer reaction to oxygen dissolved in the electrolyte, which occupies part of the free Au surface and involves also mass transport to and from the interface. It seems probable that such masking of sites and vigorous mass transport compete for adhesion sites of proteins. Finally, the accumulation of Ca^{2+} near the interface at alkaline pH may lead to local concentrations exceeding the solubility product of $Ca(OH)_2$ which may precipitate and block the surface. This is currently under intensive EQMB investigation in respect to other buffer solutions of practical importance in the recrystallization of S-layers.

When the double layer becomes neutral at the *pzc* (−0.8 V), the surface excess of cationic and anionic charges becomes equal, the S-layer form a homogeneous distribution of smaller monolayer clusters with diameters around 50 nm and heights of 4.6 nm (Fig. 3b and c). Obviously, this surface condition gives rise to a higher number of nuclei that shows a limited growth. According to Fig. 1, also in this potential range, the oxygen reduction is predominant, and may affect the surface binding of the protein molecules.

In the positively charged *dl*-region with the anion excess at −0.2 V, the S-layer units can compete with any other species very successfully and can form homogeneous polycrystalline 2D-monolayers (Fig. 3d). In this potential range, the electrode is ideally polarized with no net charge transfer in parallel. The positively charged Au surface atoms interact with negative chemical functions, i.e. the $-COO^{-}-$ groups and can replace their counterions such as Na^{+} or even Ca^{2+}, which are strongly repulsed from the interface.

The situation abruptly changes when the potential is shifted into the oxide monolayer region at +0.4 V (Fig. 3e). According to fixation experiments on oxide-covered silicon wafers one should expect good bonding condition. Actually, S-layer units practically cannot adhere and no 2D-crystals could be observed, because the applied potential is already in a region where peptides and proteins undergo oxidation. That means that those protein functional groups

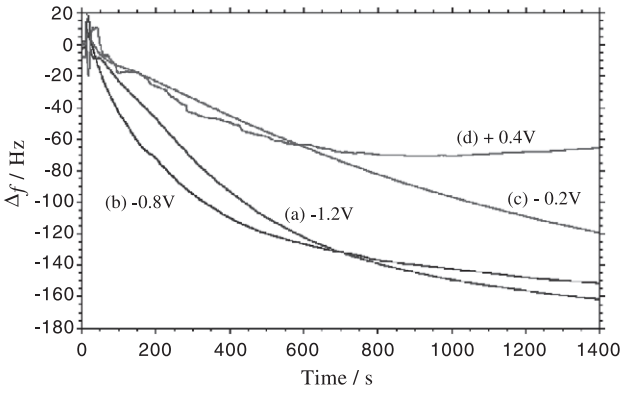

Fig. 4. In-situ EQMB measurements of S-layer recrystallization. Borate buffer with $Ca(ClO_4)_2$, pH 9. Potentials (vs. MSE): (a) −1.2 V; (b) −0.8 V; (c) −0.2 V; (d) +0.4 V. Δf: EQMB frequency change.

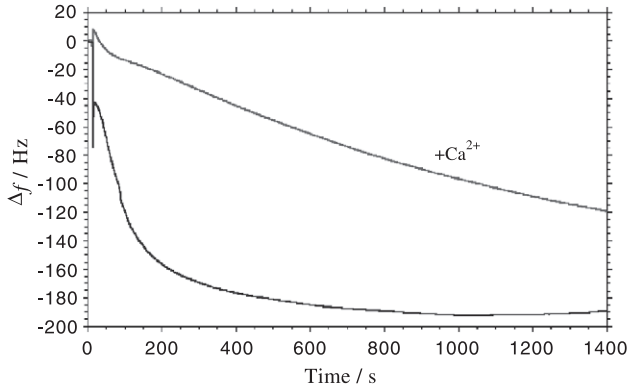

Fig. 5. In-situ EQMB measurements of S-layer recrystallization. Borate buffer with/without $Ca(ClO_4)_2$, pH 9. Potential (vs. MSE): −0.2 V. Δf: EQMB frequency change.

involved in a possible fixation on Au are irreversibly changed.

In-situ investigations allowed monitoring the time evolution of the recrystallization steps in contrast to the emersion experiments in combination with ex-situ SFM, which only provide information of the final steady state. In-situ EQMB transients have been recorded after the addition of S-layer protein unit solution into the buffer electrolyte (Fig. 4). The frequency decrease corresponding to mass increase observed in the positive *dl*-region at −0.2 V showed the slowest transient (Fig. 4c). According to the above findings this can be related to the formation of a monolayer of S-layer (comp. Fig. 3d). At the *pzc* (Fig. 4b) and negative of the *pzc* (Fig. 4a), the mass increases faster due to a highly inhomogeneous deposition (comp. Figs. 2 and 3a–c). Finally, the deposition in the oxide region levels off much quicker (Fig. 4d) according to the electrochemical instability of the S-layer.

Ca^{2+} cations are added to the borate buffer to serve as a bivalent lateral linking agent for S-layer protein monomer so that 2D-crystals are preferentially formed. These Ca^{2+} cations function as salt bridges between two negatively charged side groups (e.g. $-COO^-$) on the S-layer protein. Its presence, however, affects the vertical immobilisation kinetics. When Ca^{2+} is not employed, the adsorption of the protein units takes place much faster and is complete already after about 10 min (Fig. 5). In the presence of Ca^{2+} the monolayer formation is retarded (Fig. 4). It already forms salt bridges in the bulk of the solution so that larger agglomerates already exist which diffuse to the surface and have to undergo longer adsorption/desorption steps until they arrange in a homogeneous 2D-lattice. This crystallization process is obviously faster when only S-layer units adsorb which stay less laterally bonded without the linking agent (Fig. 5a,b).

An important result was that the protein monolayer could be formed in borate buffer of pH 9 in much less than one hour in contrast to several hours common in typical self-assembled monolayer generation. The theoretical calculation of the frequency shift due to the monolayer formation of SbpA protein on the gold substrate gives a value of 510 ng cm^{-2}, (102 ng on active area 0.2 cm^2 corresponding to $\Delta f = 76$ Hz). According to this appreciation, a monolayer should be reached before ~5 min without Ca^{2+} and after 10 min with Ca^{2+} ions under potential control in the positive *dl* region (Fig. 5).

The in-situ EQMB time evolution were supported by XPS investigation of emersed electrodes. C1s, O1s, N1s, and

Table 2
XPS results for emersed electrodes: time-evolution of S-layer crystallization on Au

Immersion time (s)	Surface scan	C1s	O1s	N1s	Au4f$_7$
0	C: 53% O: 7.5% Au: 35% S: 4.5%	284.7 → a–C (55,793) 286 → C–S/C–O (9966)	532 → –OH (hydroxides) (14,457) 533 → C=O (12,513)	–	84 → Au–Au/–Au–CH_2...(288,806)
30	C: 56% O: 11% Au: 33%	284.9 → a–C (58,580) 285.8 → C–O (9850) 287.5 → C=O (4913)	531.7 → –OH (hydroxides) (17,798) 532.9 → C=O (17,747)	–	84 → Au–Au/–Au–CH_2... (280,062)
120	C: 46.5% O: 34.5% N: 9% Au: 1.5%	285 → a–C (80,398) 286.5 → C–N (29,069) 288.5 → C=O (22,241)	532.2 → –OH (O...HOH) (56,676) 533.2 → C=O (52,068)	400.3 → C–N (peptide) (35,491)	84 → Au–Au/– Au–CH_2... (86,276)
600	C: 47% O: 34% N: 8.5% Au: 1.5%	285.1 → a–C (70,776) 286.6 → C–N (20,818) 288.6 → C=O (17,670)	532.2 → –OH (O...HOH) (37,011) 533.3 → C=O (43,910)	400.4 → C–N (peptide) (35,707)	84 → Au–Au/–... Au–CH_2... (77,412)

Emersion potential: −0.2 V_{MSE}. Electrolyte: 100.5 mM Na^+, 120 mM ClO_4^-, 1 mM borate, 10 mM Ca^{2+}, 0.001 mM S-layer. Numbers in brackets: signal values in normalized arbitrary units.

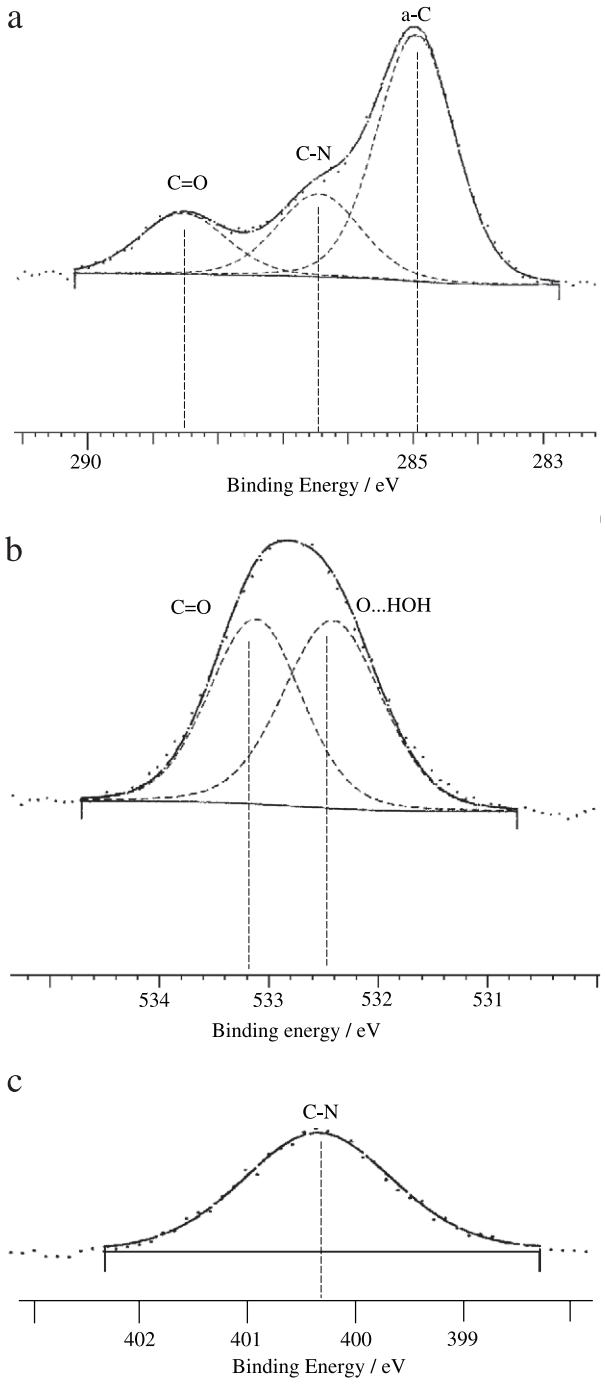

Fig. 6. Representative XPS spectra of C1s (a), O1s (b), N1s (c) of gold electrodes after S-layer recrystallization processing (120 s). Emersion potential (vs. MSE): − 0.2 V.

Au4f spectra were recorded at electrodes emersed at − 0.2 V after 30, 120 and 600 s, after protein unit addition to the electrolyte (Table 2). A reference sample was also analysed, which served as comparison with the emersed electrodes in order to discriminate the influence of the surface contaminants, usually C and O, from the S-layer contribution.

A typical C1s spectrum of a crystalline S-layer on gold shows three peaks. The binding energy (*BE*) of ~ 285 eV represents the CH_2-backbone, the *BE* ~ 286.5 eV and ~ 288.5 eV the typical peptide C–N bonds, and the C=O carboxylate binding sites, respectively (Fig. 6a). The deconvolution of the O1s signal shows a *BE* at 532.2 eV due to O...HOH bonds (hydrogen bridges) and at 533.2 eV

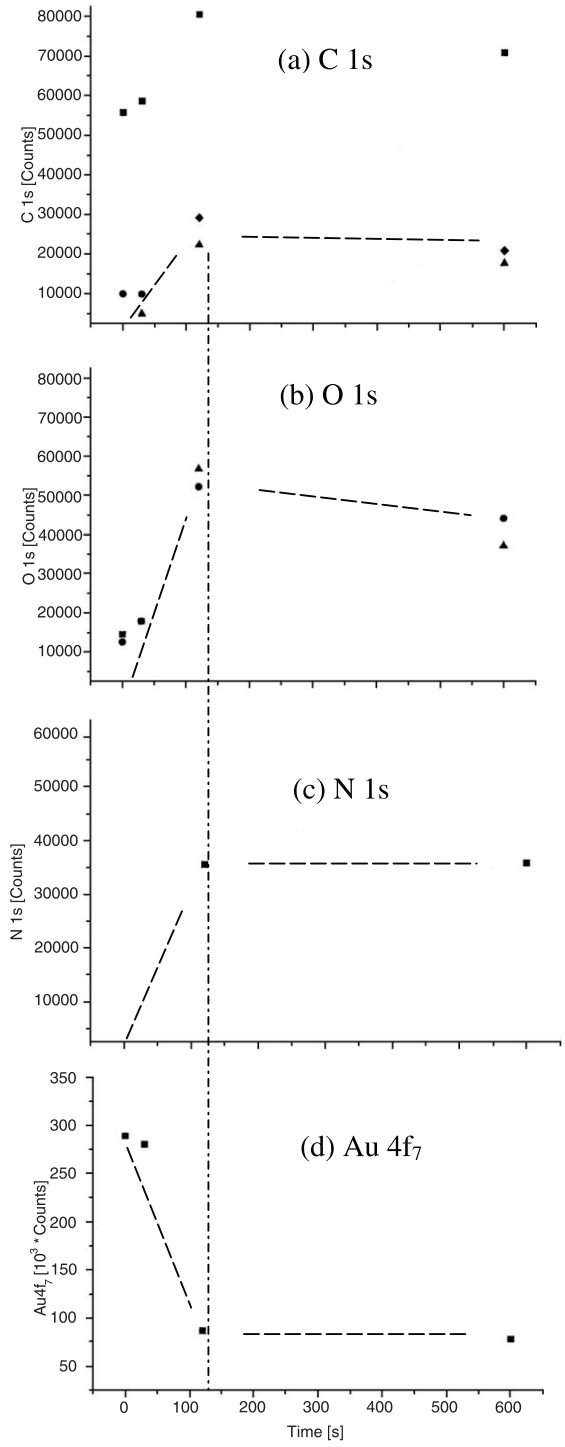

Fig. 7. XPS–time evolution of the S-layer recrystallization on gold. Emersion potential − 0.2 V (vs. MSE): (a) C 1s: ■ a–C, ● C–O, ▲ C=O, ◆ C–N; (b) O 1s: ■ –OH, ▲ O...HOH, ● C=O; (c) N 1s: ■ C–N (peptide); (d) $Au4f_7$: ■ Au–Au/–Au–CH_2–.

corresponding to C=O (carboxylate binding sites) consistent with the C1s peak at 288.5 eV (Fig. 6b). The N1s peak (Fig. 6c) centred at 400.3 eV is indicative for N in the peptide bonds consistent with the C1s peak at 286.5 eV.

The XPS time-evolution results are summarized in Fig. 7. The C1s and N1s signals directly related to peptide bond C–N increase up to c. 130 s and level off above. The Au4f signal behaves complementary because it is shielded by the S-layer. Also the other bonds that may not only be derived from proteins but also from foreign contaminants show an analogous trend. This suggests a saturation of protein coverage after even 2 min.

4. Summary

This study demonstrated that the recrystallization and fixation of 2D-crystalline S-layers on an electronic conductor can be influenced and controlled by direct electrochemical manipulation. Thus, bond formation between protein molecules and surface atoms could be accelerated or blocked.

In the positively charged electrochemical double layer region positive of the point of zero charge with anion excess, the S-layer units can compete with any other surface adsorbates very successfully and can form homogeneous polycrystalline 2D-monolayers. The positively charged Au surface atoms can interact with carboxylate groups on the protein molecule.

In the negatively charged electrochemical double layer region with cation excess negative of the point of zero charge, S-layer units cannot form homogeneous monolayer crystals. Instead, isolated multilayer clusters arranged around few nucleation sites. The reduction of oxygen traces may compete for bonding sites and the accumulation of Ca^{2+} near the interface at alkaline pH may lead to local concentrations exceeding the solubility product of $Ca(OH)_2$ which may precipitate and block the surface.

The gold oxide monolayer region is beyond the electrochemical stability of peptides and proteins so that bonding sites on the biomolecules are irreversibly changed and hinder binding to the electrode surface.

In-situ electrochemical quartz microbalance investigations together with ex-situ XPS measurements on emersed S-layer samples allowed monitoring the time evolution of the recrystallization steps. The deposition rate depends on the potential and the presence of the linking agent Ca^{2+}. The protein S-layer formation on the gold electrodes can take place within few minutes in contrast to hours common in self-assembled monolayer (SAM) generation.

Acknowledgements

This work was partially funded by the European Information Societies Technology (IST) programme project, Contract No. IST-1999-13478, and by the German Science Foundation (DFG Schwerpunktprogramm ‘‘Grundlagen der Elektrochemischen Nanotechnologie’’). The authors would like to thank D. Treu (Laboratory VIII.23 ‘‘Surface and Thin Film Analysis’’) for running XPS measurements.

References

[1] U.B. Sleytr, P. Messner, P. Pum, D. Pum, M. Sára, Angew. Chem., Int. Ed. 38 (1999) 1034.
[2] S. Dieluweit, D. Pum, U.B. Sleytr, Supramol. Sci. 5 (1998) 15.
[3] A. Neubauer, S. Pentzien, S. Reetz, W. Kautek, D. Pum, U.B. Sleytr, Sens. Actuators 40 (1997) 231.
[4] P. Pum, A. Neubauer, U.B. Sleytr, S. Pentzien, S. Reetz, W. Kautek, Ber. Bunsenges. Phys. Chem. 101 (1997) 1686.
[5] A. Neubauer, W. Kautek, S. Dieluweit, D. Pum, M. Sahre, C. Traher, U.B. Sleytr, PTB-Berichte F-30 (1997) 149.
[6] M. Sahre, S. Reetz, B. Lindner, A. Medovic, U.B. Sleytr, A. Neubauer, W. Kautek, PTB-Bericht F-39 (2000) 8.
[7] P. Messner, D. Pum, M. Sara, in: U.B. Sleytr (Ed.), Crystalline bacterial cell surface proteins, R.G. Landes Comp., Austin and Academic Press, San Diego, 1996, p. 175.
[8] D. Pum, U.B. Sleytr, Supramol. Sci. 2 (1995) 193.
[9] D. Pum, A. Neubauer, E. Györvary, M. Sara, U.B. Sleytr, Nanotechnology 11 (2000) 100.
[10] W. Kautek, M. Sahre, D.M. Soares, Ber. Bunsenges. Phys. Chem. 99 (1995) 667.
[11] W.H. Hansen, D.M. Kolb, J. Electroanal. Chem. 100 (1979) 493.
[12] W. Kautek, J.G. Gordon, J. Electrochem. Soc. 137 (1990) 3405.
[13] B. Wetzer, D. Pum, U.B. Sleytr, J. Struct. Biol. 119 (1997) 123.